Controllable coupling between flux qubit and nanomechanical resonator by magnetic field

2007 New J. Phys. 9 35

(http://iopscience.iop.org/1367-2630/9/2/035)

New Journal of Physics
The open-access journal for physics

Controllable coupling between flux qubit and nanomechanical resonator by magnetic field

Fei Xue[1,3], Y D Wang[1], C P Sun[1], H Okamoto[2], H Yamaguchi[2] and K Semba[2]

[1] Institute of Theoretical Physics, Chinese Academy of Sciences, Beijing 100080, People's Republic of China
[2] NTT Basic Research Laboratories, NTT Corporation, Atsugi-shi, Kanagawa 243-0198, Japan

New Journal of Physics **9** (2007) 35
Received 15 July 2006
Published 21 February 2007
Online at http://www.njp.org/
doi:10.1088/1367-2630/9/2/035

Abstract. We propose an active mechanism for coupling the quantized mode of a nanomechanical resonator to the persistent current in the loop of a superconducting Josephson junction (or phase slip) flux qubit. This coupling is independently controlled by an external coupling magnetic field. The whole system forms a novel solid-state cavity quantum electrodynamics (QED) architecture in the strong coupling limit. This architecture can be used to demonstrate quantum optics phenomena and coherently manipulate the qubit for quantum information processing. The coupling mechanism is applicable for more generalized situations where the superconducting Josephson junction system is a multi-level system. We also address the practical issues concerning experimental realization.

[3] Author to whom any correspondence should be addressed.

PII: S1367-2630(07)28751-8

Contents

1. Introduction

In recent years, great advances in improving the coherence of superconducting qubits have made them promising candidates for the physical realization of quantum information processing. Single qubit Rabi oscillation and Ramsey fringe have been observed and two qubit entanglement has also been achieved. Meanwhile, as an artificial two-level atom, a superconducting qubit is adjustable (e.g. by flux, bias voltage, etc) and scalable. These features are favourable for quantum state engineering. A number of protocols have been proposed to engineer the superconducting qubit to form a quantum network. Among them, a very intriguing and successful example is the circuit quantum electrodynamics (QED) architecture [1]. By coupling the cooper pair box (charge qubit) to the quantized field of a coplanar superconducting transmission line, a macroscopic solid-state analogue of cavity QED is realized on chip. Most recently, vacuum Rabi oscillations have been observed in a coupling system of a 3 Josephson junction (3-JJ) flux qubit and LC circuit [2]. Quantum optical phenomena in traditional cavity QED can be demonstrated in this solid-state composite system. Furthermore, due to its special structure, it offers a number of advantages, such as strong coupling and easy controllability. Thus, some protocols that could not be realized previously in optical cavity QED have now become possible [3, 4].

The circuit QED experiments motivate us to investigate the possibility of substituting other quantum solid-state devices for the transmission line. It is very desirable to couple a Josephson junction qubit to a device with low energy consumption and small size. If the strong coupling and easy controllability can also be achieved, we get another favourable cavity QED structure. A possible candidate for this solid-state device is the nanomechanical resonator (NAMR). NAMRs of GHz oscillation have already been observed. It is supposed that the NAMR enter the quantum regime at the attainable temperature of the dilution refrigerator. Schemes for coupling a Josephson charge qubit or phase qubit to a NAMR have already been proposed. Based on

these coupling mechanisms, several quantum state engineering protocols have been put forward [5]–[9]. However, due to the difficulty in reaching quantum regime of NAMR, those protocols have not been implemented experimentally yet. On the other hand, the coupling mechanism of NAMR and a flux qubit is also an attractive problem since the flux qubit is supposed to have longer coherence time as it is less affected by the charge fluctuation in the structure. To the best of our knowledge, this has not been studied in detail previously. Here, we present a novel mechanism of coupling a NAMR to a flux qubit. As we present below, the coupling strength between the NAMR and the flux qubit can be adjusted conveniently by a coupling magnetic field and turned on and off within the coherence time of the flux qubit. Since the coupling magnetic field is independent of the single qubit operation, it is possible to make it strong enough even for GHz oscillation. Therefore, using our proposal it is in principle possible to approach the 'strong coupling regime' of cavity QED at attainable temperatures of a dilution refrigerator. This coupling system acts as an analogue of a cavity QED system with more flexibility. We expect that it will enable various applications to quantum information processing and quantum state engineering.

This paper is organized as follows: in section 2, we briefly review the set-up of a 3-JJ flux qubit and NAMR as well as their experimental progress. Then we get into the coupling mechanism for a flux qubit and NAMR. This coupling mechanism can be equally applied to a rf superconducting quantum interference device (SQUID) flux qubit and a phase slip flux qubit. In section 3, the spectrum of the coupling system is presented in the 'weak coupling' and the 'strong coupling' limits respectively. The readout and quantum nondemolition (QND) measurement for the flux qubit is studied in section 4. We also consider the application of this coupling mechanism in quantum computation in section 5 and generalize the coupling system to beyond the spin-boson model in section 6. The possible problems on experimental realization and their solutions are given in section 7. In section 8, some discussions and remarks are included.

2. Coupling NAMR and flux qubit by a transverse magnetic field

2.1. The 3-junction flux qubit

A Josephson charge qubit system has been used to couple with NAMR. Here, we study another superconducting qubit system—a 3-JJ flux qubit [10]–[14]. In contrast with charge qubits, the flux qubit is far less sensitive to charge fluctuations. Estimations show that flux qubits have a relatively high quality factor [11, 13]. The configuration of a flux qubit consists of a superconducting loop with three Josephson junctions, and the Josephson coupling energy is much larger than the charging energy for each junction. The quantum state of this system is mainly determined by the phase degree of freedom. The Josephson energy of the three Josephson junction loop reads

$$U(\varphi_1, \varphi_2) = -E_J \cos\varphi_1 - E_J \cos\varphi_2, -\alpha E_J \cos(2\pi f - \varphi_1 - \varphi_2), \tag{1}$$

where the constraint of fluxoid quantization has already been taken into account. Here, E_J is the Josephson coupling energy of two identical junctions and φ_1, φ_2 are phase differences across the two junctions respectively. The Josephson energy of the third junction is αE_J, $f = \Phi_f/\Phi_0$ with Φ_f the external flux applied in the loop and $\Phi_0 = h/2e$ the flux quantum. In the vicinity of $f = 0.5$, if $\alpha > 0.5$, a double-well potential is formed within each $2\pi \times 2\pi$ cell in the phase plane and the two lowest stable classical states have persistent circulating

currents $I_p = 2eE_J\sqrt{1-(1/2\alpha)^2}/\hbar$ with opposite directions. Therefore, the flux qubit is also called a persistent current qubit. Within the qubit subspace spanned by $\{|0\rangle, |1\rangle\}$ ($|0\rangle$ and $|1\rangle$ denote clockwise and counterclockwise circulating states respectively), the Hamiltonian of the qubit system reads as

$$H_f = \omega_f \sigma_z + \Delta\sigma_x = \Omega\tilde{\sigma}_z, \tag{2}$$

where $\omega_f = I_p\Phi_0(f-0.5)$ is the energy spacing of the two classical stable states and Δ is the tunnelling splitting between the two states, $\Omega = \sqrt{\omega_f^2+\Delta^2}$ and $\tilde{\sigma}_z = \cos\theta\sigma_z + \sin\theta\sigma_x$, $\tan\theta = \Delta/\omega_f$. The offset of f from 0.5 determines the level splitting of the two states and the barrier for quantum tunnelling between the states strongly depends on the value of α. If the third junction is replaced by a dc SQUID, both f and α are tuneable in experiments by the applied flux or the microwave current [10, 11].

2.2. The NAMR

The flexural modes of thin beams can be described by the so-called Euler–Bernoulli equations [15]. In our proposal only the fundamental flexural mode of the NAMR is taken into account. All the other modes have a much smaller coupling to the flux qubit and can be neglected [16, 17]. In this case, the NAMR is modelled as a harmonic oscillator with a high-Q mode of frequency ω_b. The Hamiltonian without dissipation reads [6, 7]

$$H = \frac{p_z^2}{2m} + \frac{1}{2}m\omega_b^2 z^2. \tag{3}$$

In pursuing the quantum behaviour of a macro scale object the nano scale mechanical resonator plays an important role. At sufficiently low temperature the zero-point fluctuation of the NAMR will be comparable to its thermal Brownian motion. The detection of zero-point fluctuations of the NAMR can give a direct test of Heisenberg's uncertainty principle. With a sensitivity up to 10 times the amplitude of the zero-point fluctuation, LaHaye *et al* [18] have experimentally detected the vibrations of a 20 MHz mechanical beam of tens of micrometres size. For a 20 MHz mechanical resonator its temperature must be cooled below 1 mK to suppress the thermal fluctuation. For a GHz mechanical resonator a temperature of 50 mK is sufficient to effectively freeze out its thermal fluctuation and let it enter the quantum regime. This temperature is already attainable in dilution refrigerators.

The lithographic technology for NAMR is rather mature. The important advantages of NAMR are the potentially higher quality factor and frequency comparable to superconducting qubits. Since the early demonstration of a radio frequency mechanical resonator at Caltech [19], great advances have been made. The attainable frequencies for the fundamental flexural modes can reach 590 MHz for the doubly-clamped SiC mechanical resonator of size $1 \times 0.05 \times 0.05\,\mu$m [20] and 1 GHz oscillation frequency has also been measured [21]. It is argued that quantized displacements of the mechanical resonator were observed despite some opposite opinions [22]. For a 1 μm beam a quality factor Q of 1700 has been observed at a frequency of 110 MHz [23]. In a carefully designed antenna shape, Gaidarzhy *et al* [24] have achieved $Q = 11\,000$ for 21 MHz oscillation at the temperature of 60 mK and $Q = 150$ for 1.49 GHz oscillation at the temperature of 1 K with a comparatively large double clamped beam. The significantly small size ($\sim\mu$m) of the NAMR is also favourable for incorporating it in the superconducting qubit circuit.

2.3. The composite system with tuneable coupling

To achieve a 'strong' interaction, the coupling dynamical variable should usually be the dominant one in the dynamics of the composite system. For the Josephson phase qubit [25, 26], the phase degree of freedom dominates the dynamics and the bias current coupled with the phase is modified by the dilatational motion of the piezoelectric dilatational resonator [27]. While for the Josephson charge qubit, the coupling mechanism is that the resonator displacement modifies the effective bias charge of a Cooper-pair box [7, 8, 17, 28]. These previous investigations enlighten us to consider the coupling between the persistent current in a superconducting flux qubit loop and the motion of the NAMR.

Since the Josephson coupling energy of each junction in the flux qubit is much larger than that in the charge qubit, the persistent current in the loop could be about hundreds of nano ampere [12] in contrast with the critical current of the charge qubit (usually about 20–50 nA). The magnitude of this persistent current naturally leads us to consider the magnetomotive displacement actuation and sensing technique [15, 19]. It is well known that when a current passes through a beam of conducting material, the perpendicular arrangement of an external magnetic field and the direction of the current generates a Lorentz force in the plane of the beam. This is just the actuation part of the magnetomotive technique. Meanwhile, the resulting displacement of the beam under the Lorentz force generates an electromotive force, or voltage, which serves as measurement. Thus, if a doubly-clamped nano beam coated with superconducting material is incorporated in the superconducting qubit loop, the persistent current induces a Lorentz force with opposite directions for clockwise and counterclockwise current. The oscillation of the NAMR is modulated by these Lorentz forces. In this way, the quantized harmonic oscillation mode of the beam is coupled to the quantum state of the flux qubit system. This is just the coupling mechanism considered in our paper.

Our proposal is illustrated in figure 1. A 3-JJ system is fabricated on the x–y plane. The external applied magnetic flux Φ_f is enclosed in the loop modulated by the control lines (the lines are not plotted). The 4-JJ version of a flux qubit system can also be used here to allow the modulation of the effective Josephson energy of the third junction and hence the tunnelling amplitude of the two current states. One side of the loop (indicated by the thick (green) rod) is suspended from the substrate and clamped at both ends. This can be fabricated with a doubly-clamped nanomechanical beam coated with superconductor or with the superconductor itself as the mechanical resonator. A magnetic field B_0 is applied in the y-direction. As we discussed above, the circulating suppercurrent under the magnetic field generates a Lorentz force in the z-direction. The magnitude of the force is $B_0 I_p L$, with L the effective length of the resonator along the x-direction ($L = \xi L_0$ and L_0 is the actual length of the resonator, ξ a factor depending on the oscillation mode [29], for the fundamental oscillation mode of a doubly clamped beam $\xi \approx 0.8$). This force results in a forced term in the Hamiltonian, which reads $H_{\rm fb} = Fz = B_0 I_p L z$. With the two-level approximation of a 3-JJ loop and the single-mode boson approximation, the coupling is written as

$$H_{\rm fb} = g(a + a^\dagger)\sigma_z, \tag{4}$$

for $z \sim a + a^\dagger$. Here,

$$g = B_0(t) I_p L \delta_z \tag{5}$$

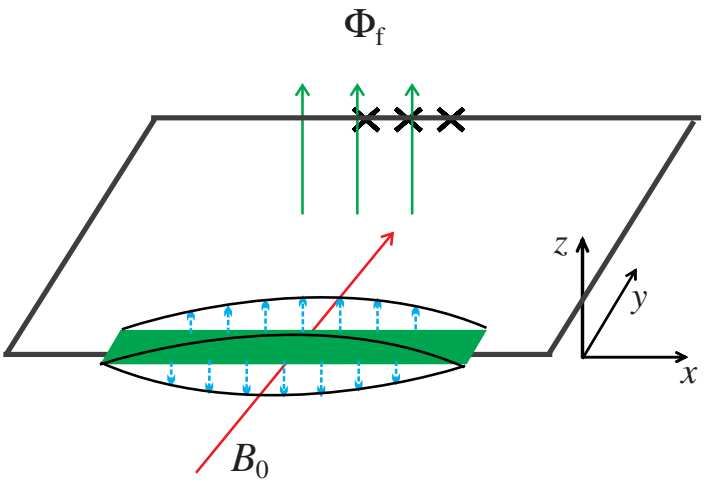

Figure 1. A 3-JJ flux qubit loop is located in the x–y plane and a NAMR is integrated in the loop (indicated by a green box). The z-direction oscillation of the NAMR couples to the current in the flux qubit loop by a transverse magnetic field B_0 in the y-direction. Another tuneable magnetic flux Φ_f penetrating this loop tunes the free Hamiltonian of the 3-JJ system.

and $\delta_z = \sqrt{\hbar/2m\omega_b}$ is the amplitude of zero-point motion in the z-direction of the NAMR, with m the effective mass of the resonator, ω_b the frequency of the fundamental flexural mode; a ($a^\dagger$) is the creation (annihilation) operator of the mode of the flexural motion in the z-direction. $\sigma_z = |0\rangle\langle 0| - |1\rangle\langle 1|$ is the Pauli matrix defined in the basis of $\{|0\rangle, |1\rangle\}$. We see that this interaction H_{fb} actually couples the two systems. Together with the free Hamiltonian of flux qubit and NAMR, the Hamiltonian of the whole system reads

$$H = \omega_b a^\dagger a + \omega_f \sigma_z + \Delta\sigma_x + g(a + a^\dagger)\sigma_z. \tag{6}$$

An important advantage of this coupling mechanism is the convenient controllability. As seen from equation (5), the coupling constant is directly dependent on the applied coupling magnetic field B_0. Thus, both the magnitude and sign of the coupling constant can be modified. What is more important is that the control parameter B_0 in the coupling coefficient equation (5) is independent of the parameters of the free Hamiltonian, such as bias voltage and external magnetic flux Φ_f. This means the free Hamiltonian and the interaction Hamiltonian can be manipulated independently. This full controllability is a rather favourable feature for quantum state engineering and quantum information processing protocols. This is in contrast with the coupling of a charge qubit and NAMR, where the coupling strength is controlled by the bias voltage which is also the crucial parameter to determine the energy spacing of the charge qubit. For example, for bang–bang cooling of NAMR by a charge qubit [8], the bias voltage should be set to a certain value to induce desirable damping. Therefore the on-and-off of the interaction between the qubit and NAMR can only be approximately controlled by detuning and this can result in harmful reheating of the NAMR. But in our present coupling mechanism, both the coupling coefficient and the energy spacing are independent. Thus, this 'bang–bang' cooling protocol should be implemented more reliably by the flux qubit and the NAMR with the above coupling mechanism.

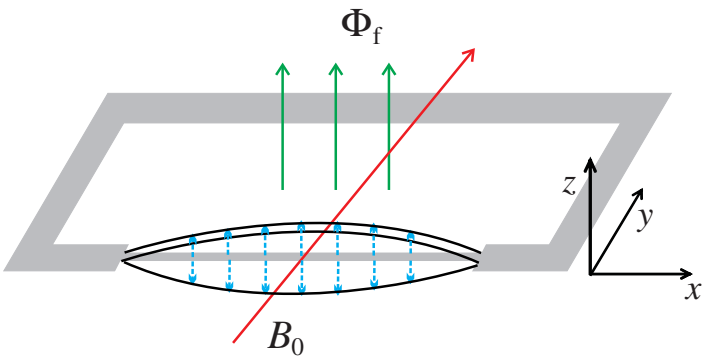

Figure 2. A superconducting narrow wire in the loop acts as the centre of a phase slip flux qubit and a NAMR.

To estimate the coupling strength, we use the following parameters in [7, 30, 31]: $I_p = 660\,\text{nA}$, $L_0 = 3.9\,\mu\text{m}$, $\omega_b = 100\,\text{MHz}$, $\delta_z = 2.6 \times 10^{-13}\,\text{m}$, $Q = 2 \times 10^4$ and assume the applied magnetic field to be $B_0 = 5\,\text{mT}$. Then we have $g \approx 4.01\,\text{MHz}$. Hence we see that the 'strong coupling' regime for cavity QED is potentially realizable in our scheme. This regime requires that the period of the Rabi oscillation $1/g$ is much shorter than both the decoherence time $1/\gamma$ of the two-level system and the average lifetime $1/\kappa = Q/\omega_b$ of the 'photon' in the 'cavity' [32]. For this composite system, the decoherence time for the flux qubit is 1–10 μs and the cavity lifetime is about 200 μs, while the Rabi oscillation time 0.016 μs is much shorter than the two lifetime scale. For GHz oscillation, the quality factor is rather low [24] (1.49 GHz with $Q = 150$), this corresponds to a much shorter cavity lifetime (about 0.1 μs). However, the coupling strength can be increased by using a larger coupling magnetic field. For example, if we take $B_0 = 50\,\text{mT}$, the Rabi oscillation period $1/g \approx 0.016\,\mu\text{s}$ which is still short enough to reach the 'strong coupling regime'. Therefore, this protocol might be promising in dilution refrigerators (several tens of millikelvin).

2.4. Phase slip flux qubits and NAMR

Most recently, a new type of flux qubit—the phase slip flux qubit—has been proposed based on coherent quantum phase slip [33, 34]. A phase slip flux qubit is formed by a high-resistance superconducting thin wire instead of the Josephson junctions. The computational basis are also the two opposed persistent current states. Our coupling scheme can be equally applicable to this type of flux qubit. There are two important advantages to consider for phase slip flux qubits. Firstly, since the superconducting thin wire can be fabricated by a suspended carbon nanotube, it acts as the phase slip centre and the NAMR simultaneously. The circuit configuration is simplified (see figure 2). Secondly, if one uses this qubit, one can be free from any fluctuation due to imperfection or two-level systems hidden in the dielectric layer of the Josephson junction.

3. Energy spectrum of coupling system

The Larmor frequency of a superconducting qubit is about the order of 10 GHz, while the frequency of NAMR only reaches several hundred MHz with quality factor 10^4 at the present

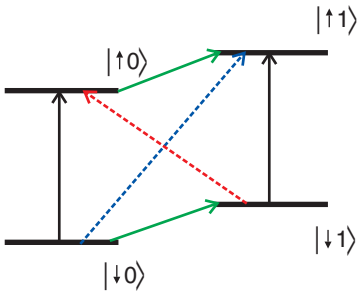

Figure 3. The dressed energy levels and transition diagram for the weakly coupled system.

stage. Thus, the composite system of flux qubit and NAMR is in the large detuning regime of cavity QED, i.e., the following condition is satisfied

$$\frac{g}{|\Omega - \omega_b|} \ll 1. \tag{7}$$

However, the superconducting flux qubit and the NAMR are non-resonant, i.e. $\Omega \gg \omega_b$. This is in contrast with Yale's circuit QED experiment where the Cooper pair box is resonant with the one-dimensional (1D) transmission line [35]. In the following, we discuss the energy spectrum of our model in two different regimes: $g \ll \omega_b$ (denoted as 'weak coupling') and $g \approx \omega_b$ (denoted as 'strong coupling'). In our proposal, the two regimes can be reached by varying the applied coupling magnetic field B_0; the energy spectra are qualitatively different from each other. It is notable that [36] has proved that the dispersive measurement back action can be enhanced or reduced by cavity damping respectively in the two regimes.

3.1. 'Weak coupling' and sideband spectrum

For the parameters $B_0 = 5\,\mathrm{mT}$, $g = 4.01\,\mathrm{MHz}$, both g/Ω and g/ω_b are much smaller than 1. In this case, the energy spectrum can be calculated by the Floquet approach or by Frölich transformation. After performing a unitary transformation on the original Hamiltonian (6), we get the effective Hamiltonian

$$H_{\mathrm{eff1}} \approx \omega_b a^\dagger a + \Omega\tilde{\sigma}_z + \mathrm{i}\frac{g^2 \sin 2\theta}{\omega_b}(a^2 - a^{\dagger 2})\tilde{\sigma}_y + \frac{g^2 \sin\theta}{\Omega}(a + a^\dagger)^2(\cos\theta\tilde{\sigma}_x + \sin\theta\tilde{\sigma}_z). \tag{8}$$

The spectra are $n\omega_b + m\Omega$ plus some small off-diagonal transition terms that are of order $O(g/\omega)$ or $O(g/\Omega)$. As shown in figure 3, the energy levels of the two subsystems are weakly perturbed by the coupling due to the large detuning. By applying a microwave pulse to induce the transition between those levels, the blue sideband ($|00\rangle \rightarrow |11\rangle$) and red sideband transitions ($|01\rangle \rightarrow |10\rangle$) can be observed in addition to the main zero-photon transition $|00\rangle \rightarrow |10\rangle$ [37]. This atomic physics phenomenon has already been observed in a solid quantum system of a flux qubit and a dc SQUID oscillator [38]. For our proposal, similar spectra are expected.

3.2. *'Strong coupling' and dispersive shift*

With large magnetic field, for example, $B_0 = 100\,\mathrm{mT}$, then $g = 80.2\,\mathrm{MHz}$. The magnitude of coupling is comparable to the characteristic energy scale of the NAMR. In this case, the coupling term is not a perturbation with respect to the free Hamiltonian of NAMR. Therefore, we cannot use perturbation theory. However, since the large detuning condition is still held, we resort to adiabatic elimination (or coarse-graining technique) to deal with this problem. Since $\Omega \gg \omega_\mathrm{b}$, the energy spectrum of the whole system is roughly energy band structure. Then the spacing of bands is determined primarily by Ω and the energy spacing within each band is approximately ω_b. By adiabatic elimination of the transition between different bands, we can obtain the effective Hamiltonian from equation (6)

$$H = H_e \left|e\right\rangle \left\langle e\right| + H_g \left|g\right\rangle \left\langle g\right|, \tag{9}$$

where the two-component Hamiltonians are

$$H_{e,g} = \omega_{e,g} A_{e,g}^\dagger A_{e,g} \pm \Omega - g^2 \cos^2\theta \frac{\omega_\mathrm{b}}{\omega_{e,g}^2}, \tag{10}$$

with the frequencies

$$\omega_{e,g}^2 = \omega_\mathrm{b}^2 \mp \frac{4g^2\omega_\mathrm{b}\sin^2\theta}{\Omega - \omega_\mathrm{b}}, \tag{11}$$

and the new bosonic operators $A_{e,g}$ are defined by

$$A_{e,g} = \mu_{e,g} a + \nu_{e,g} a^\dagger + \eta_{e,g}. \tag{12}$$

In the above equation

$$\mu_{e,g} = \sqrt{\frac{\omega_{e,g}}{4\omega_\mathrm{b}}} + \sqrt{\frac{\omega_\mathrm{b}}{4\omega_{e,g}}}, \tag{13a}$$

$$\nu_{e,g} = \sqrt{\frac{\omega_{e,g}}{4\omega_\mathrm{b}}} - \sqrt{\frac{\omega_\mathrm{b}}{4\omega_{e,g}}}, \tag{13b}$$

$$\eta_e = \frac{g\cos\theta\sqrt{\omega_\mathrm{b}\omega_e}}{\omega_e^2}, \tag{13c}$$

$$\eta_g = -\frac{g\cos\theta\sqrt{\omega_\mathrm{b}\omega_g}}{\omega_g^2}. \tag{13d}$$

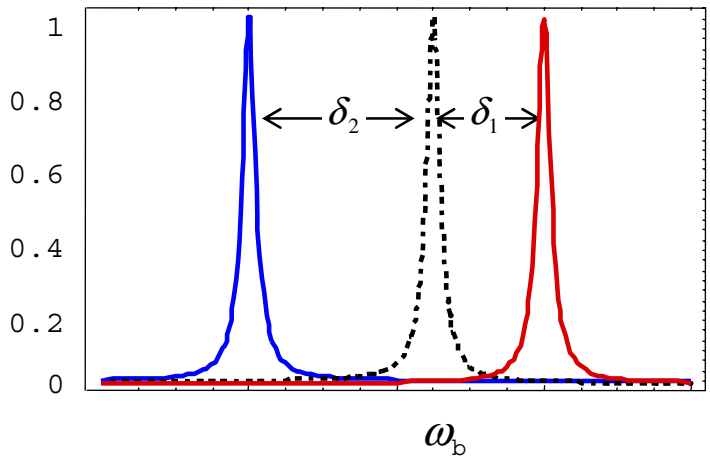

Figure 4. Dispersive 'pull' of the frequency of NAMR with asymmetric shifts from its original frequency.

Thus, for different states of the flux qubit, the energy spectrum of the NAMR is shifted by different values, or in other words, the flux qubit pulls the cavity frequency by δ_1 and $-\delta_2$ (see figure 4) with

$$\delta_1 = \sqrt{\omega_b^2 + \frac{4g^2\omega_b \sin^2\theta}{\Omega - \omega_b}} - \omega_b, \tag{14a}$$

$$\delta_2 = \omega_b - \sqrt{\omega_b^2 - \frac{4g^2\omega_b \sin^2\theta}{\Omega - \omega_b}}. \tag{14b}$$

In contrast with the dispersive limit discussed in circuit QED [1], the dispersive shift here is asymmetric.

4. QND measurement for flux qubit

Usually, the flux qubit is measured through a dc SQUID in the underdamped regime that is inductively coupled [12, 39] or directly coupled [40]–[42]. The external applied flux plus the flux induced by the persistent current decide the switching current of the dc SQUID. By ramping a bias current to the dc SQUID, the switching current can be recorded. When a continuous microwave is resonant with the level spacing of the two eigenstates of the flux qubit, the qubit is flipped and the switching current is changed. This results in peak and dip in the switching current level versus the applied flux. With this method, both the energy spectrum and the dynamic evolution have been observed. During this measurement process, the quantum information encoded in the qubit is destroyed [30]. It would be favourable to design a nondestructive and QND [43] measurement protocol. A novel phase-sensitive microwave reflection approach is now applied for the readout of superconducting qubits [30], [44]–[46]. The advantage of this method is that it directly probes the dynamics of the Josephson plasma resonance in both the linear and nonlinear regimes without

switching the detector Josephson circuit to a dissipative state. It succeeded in providing very fast and far less destructive measurement of the qubit. However, the QND readout for the flux qubit [47] only works far away from the optimal point, where the qubit coherence is destroyed very quickly.

Here, we indicate that our composite system can be used to perform QND measurement on a flux qubit. As we discussed in the previous section, in both cases, the interaction between the NAMR and the flux qubit results in the mixed energy spectrum for them. Therefore, through the spectroscopy measurement, the quantum state of one system can be detected via the spectrum of the other one. Especially, if the interaction Hamiltonian commutes with the free Hamiltonian of the measured object and does not commute with that of the measuring device, a QND measurement protocol can be implemented. This is just the case of the 'strong coupling' limit in our proposal. In this case, by the spectroscopy of the NAMR, the flux qubit state can be read out without perturbation. This can be predicted from equations (9)–(12): the frequency of NAMR is ω_e when the flux qubit is in the excited state, while its frequency is ω_g when the flux qubit is in the ground state. The interaction between the NAMR and the flux qubit commutes with the free Hamiltonian of the flux qubit. Hence the measured probabilities of eigenstates are not perturbed by this readout. Therefore, the spectroscopy measurement of NAMR provides a high resolution QND measurement on the qubit state. It should be noticed that this scheme does not work at the exact optimal point ($\sin\theta = 0$ at the optimal point). However, if the operation point is only a little bit shifted away from the optimal point, e.g. $\omega_f \approx \Delta$, the resulting frequency shift is observable (suppose $B_0 = 100\,\mathrm{mT}$, $\omega_\mathrm{b} = 100\,\mathrm{MHz}$ and $Q = 2 \times 10^4$, then $\delta_{1,2} \gg \kappa$) in the spectrum.

This frequency shift can be measured through the frequency measurement of the NAMR. In principle, this can be done with magnetomotive techniques [24, 48]. During the measurement process, a perpendicular magnetic field and oscillation current is applied on the NAMR. Then, the NAMR behaves like a frequency-dependent resistance. The largest effective resistance is obtained when the NAMR is in resonance with the oscillation current. Thus the frequency of NAMR is inferred by the resonance peak of its voltage between its two ends when we vary the frequency of the oscillation current in it. Another possible way to the frequency measurement of NAMR is to use a single-electron transistor (SET) [49]–[51]. The SET does not require extra magnetic field which might induce unwanted perturbation to the superconducting loop. It is supposed to have very high sensitivity and is expected to reach the limit by the uncertainty principle. For this method, the mechanical motion of the NAMR couples to the SET through a lead on the NAMR that is close to the island of the SET. The motion of the NAMR modulates the coupling capacitance between the lead and the SET. When there is a bias voltage on the lead of the NAMR the potential of the island near the NAMR is modulated. The frequency of the mechanical motion is detected through the conductance of the SET.

On the other hand, the measurement of high-frequency mechanical oscillators has some practical difficulties as an additional strong coupled transducer is required to convert its dynamics to electronic signals. There is an equally intriguing problem: to detect the property of the NAMR via the measurement of a superconducting qubit since there have been some good measurement protocols for the latter. For the coupling mechanism presented in this paper, the effective Josephson energy is modified by the displacement of the NAMR in a similar way to the charge energy of the SET being modified by the displacement of the NAMR. Thus, the flux qubit might be able to act as a transducer to detect the state of the NAMR. Most recently, a QND measurement for NAMR via rfSQUID has been considered based on a configuration similar to ours [52].

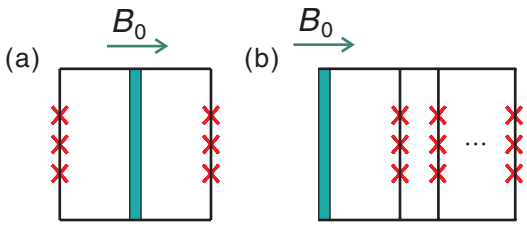

Figure 5. The NAMR couples to (a) two or (b) multiple flux qubits. The green narrow box represents the NAMR and the cross stands for the Josephson junction. The coupling is controlled by a magnetic field perpendicular to the NAMR in the coplanar of the NAMR and flux qubit.

5. Applications in quantum computation

One of the possible applications of our proposal in quantum computation is to couple two or more flux qubits together and to realize a two qubit logic gate. As shown in figure 5(a), the NAMR serves as a quantum data bus and the two identical qubit loops are connected to it. The total Hamiltonian reads

$$H = \omega_{\mathrm{b}} a^{\dagger} a + \sum_{i} [\omega_f \sigma_{zi} + \Delta \sigma_{xi} + g(a + a^{\dagger})\sigma_{zi}], \tag{15}$$

where σ_{zi} and σ_{xi} are Pauli operators for the ith flux qubit. The coupling coefficient g can be modulated by the magnetic field B_0. If we fix B_0, the parameters for manipulating single qubit (i.e., ω_f and Δ) operations are still tuneable by adjusting f and α. This offers a universal architecture to realize a coherent two qubit quantum logic gate [53]. Considering the inductance of the loop L_{p}, we note that there is also direct magnetic coupling induced by the sharing edge $L_{\mathrm{p}}(I_1 + I_2)^2/2 \sim \sigma_{z1}\sigma_{z2}$, here I_1, I_2 are the currents in the 1st and 2nd qubit loop respectively. The order of magnitude of this zz coupling is about 10–100 MHz. At the degeneracy point, this always-on coupling is commute with the whole Hamiltonian, therefore it is not very hard to deal with. Away from the degeneracy point, the direct magnetic coupling may have a positive or negative effect with respect to concrete proposals.

More qubits can also be connected in the same way as shown in figure 5(b). By the tuneable energy spacing of the flux qubit, we can selectively couple two qubits through the NAMR. With this configuration, we can realize the logic gate of two arbitrary flux qubits by adiabatic elimination or by dynamic cancellation of the NAMR cavity mode [28, 54].

6. Beyond the spin-boson model

In the above discussion, we have described our coupling mechanism in the spin-boson regime where the 3-JJ superconducting loop is treated as a quasi two-level system, i.e., a qubit. However, when the magnetic flux Φ_f is tuned away from $\Phi_0/2$, the lowest two energy levels cannot be isolated from the other energy levels (see the energy spectrum, for example, in [55]). Taking more energy levels into consideration is advantageous to investigate many intriguing phenomena that are traditionally studied in atomic physics and quantum optics. For example, with the lowest

three energy levels, stimulated Raman adiabatic passage (STIRAP) can be studied and some interesting behaviour, such as electromagnetic induced transparency (EIT) and dark states, can be exhibited in the coupling system. What is more, as the symmetry and the selection rule of the three-level superconducting loop are different from those of the three-level natural atom, some novel features can be demonstrated, for example, the Δ-type atom [56] and persistent single photon generation [57].

Our coupling protocol can also be generalized to the model of a multi-level atom in a cavity. In this case, the dynamics of the 3-JJ loop is not confined to the two-level subspace. With newly-defined variables $\varphi_{\mathrm{p}} = (\varphi_1 + \varphi_2)/2$, $\varphi_{\mathrm{m}} = (\varphi_1 - \varphi_2)/2$ and their conjugate momentum P_{p}, P_{m}, the free Hamiltonian of the 3-JJ system has a similar form to that of a particle in a 2D periodical potential [11]:

$$H_f = \frac{P_{\mathrm{p}}^2}{2M_{\mathrm{p}}} + \frac{P_{\mathrm{m}}^2}{2M_{\mathrm{m}}} + 2E_J(1 - \cos\varphi_p \cos\varphi_m) + \alpha E_{\mathrm{J}}[1 - \cos(2\pi f + 2\varphi_{\mathrm{m}})], \tag{16}$$

where $M_{\mathrm{p}} = 2C_{\mathrm{J}}(\Phi_0/2\pi)^2$ and $M_{\mathrm{m}} = M_{\mathrm{p}}(1 + 2\alpha)$, and C_{J} is the capacitance of the first and second junctions. Then the interaction Hamiltonian is still $H_{\mathrm{fb}} = B_0 I L z$ where I is the current flow through the NAMR [57]

$$I = \frac{2eC_{\mathrm{S}}E_{\mathrm{J}}}{\hbar C_{\mathrm{J}}}[2\cos\varphi_{\mathrm{p}} \sin\varphi_{\mathrm{m}} - \sin(2\pi f + 2\varphi_{\mathrm{m}})], \tag{17}$$

with $1/C_S = \sum_i 1/C_i$. The current I induces the transition between different eigenstates of the free Hamiltonian of the 3-JJ system and numerical calculation can predict the transition amplitudes. For example, if we only consider the lowest three energy levels $|0\rangle$, $|1\rangle$ and $|2\rangle$, the above Hamiltonian can be written in a 3D subspace:

$$H = \omega_{\mathrm{b}} a^{\dagger} a + \sum_i \Omega_i |i\rangle\langle i| + \lambda \sum_{i \neq j} (\Omega_{ij} |i\rangle\langle j| + \mathrm{h.c.})(a + a^{\dagger}), \tag{18}$$

where $|i\rangle (i = 0, 1, 2)$ is the ith eigen level of the 3-JJ system and Ω_i is the corresponding eigenenergy (usually we take $\Omega_0 = 0$). The coupling coefficient $\lambda = B_0(t) L \delta_z$ and $\Omega_{ij} = \langle i | I | j \rangle$. As shown in figure 6, the transition amplitudes Ω_{01}, Ω_{02} and Ω_{12} between the lowest three energy levels depend on f. That is to say, we can control the transition between different energy levels of the uncoupled system. Apparently, this feature can be used in STIRAP technology and some other proposals based on a three-level atom with a quantized field [58]. For example, when the superconducting loop is biased a little bit away from the the optimal point, a λ-type three-level atom is formed approximately. Following the same strategy of [59], replacing the lowest three energy levels of quantronium by the eigen-levels considered above, Fock-states of the NAMR can also be generated.

7. Experimental considerations

In the above discussion, we have assumed that the NAMR oscillates only in the z-direction. However, to manipulate the 3-JJ flux qubit, a bias magnetic flux Φ_f is applied through the loop in the z-direction. This bias magnetic field also induces a Lorentz force on the NAMR in

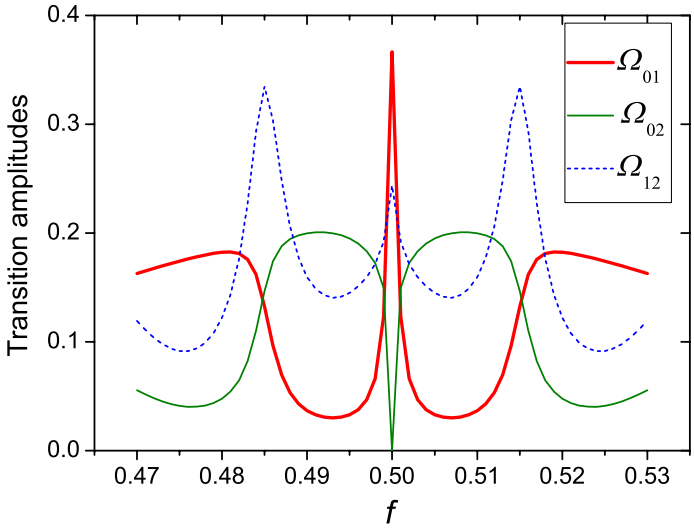

Figure 6. The transition amplitudes between the lowest three energy levels $|0\rangle$, $|1\rangle$ and $|2\rangle$ vary with the offset f.

the y-direction. Therefore there exists an always-on interaction between the flux qubit and the y-direction motion of the NAMR $H'_{\rm fb} = g'(a_y + a_y^\dagger)\sigma_z$, where a_y denotes the annihilation operator of the mode of the flexural motion in the y-direction and the coupling strength is

$$g' = \Phi_f I_{\rm p} L \delta_y / \Phi_0, \tag{19}$$

where δ_y is the zero-point fluctuation of the NAMR in the y-direction. However, since

$$\frac{g'}{g} = \frac{B_{\rm bias}}{B_0} \cdot \frac{\delta_y}{\delta_z}, \tag{20}$$

$B_{\rm bias} = \Phi_f / S$, with S the area enclosed by the loop of 3-JJ flux qubit, this additional coupling can be substantially suppressed by a properly designed asymmetric structure of the NAMR to set $\delta_y/\delta_z \ll 1$. This can be made when the dimension of the NAMR in the y-direction is larger than that of the z-direction. Then the dominant coupling is the one induced by the magnetic field B_0. The bias field for the flux qubit at $\Phi_f = 0.5\Phi_0$ is calculated as 19 μT with the loop area of [60] or 250 μT with a smaller loop of [40]. This corresponds to a coupling strength of 12 or 160 kHz (with $\delta_y = 0.1\delta_z$), which is always less than 10^{-1} of the coupling induced by the external applied magnetic field B_0 even in the 'weak coupling' situation discussed above. Therefore, this always-on coupling is negligible for B_0 stronger than 1 mT.

Another possible difficulty in experiments might come from the vibration of the sample (the substrate with the flux qubit and the NAMR on it). If the controlling magnetic field B_0 in the y-direction is generated by a coil located on another cold finger, then in general, there may exist uncontrollable relative motion of this sample cavity against the outside coil system. This relative oscillation between the coil and the sample induces the fluctuation of the controlling field. And more seriously, the torsional oscillation of the sample will cause the deviation of the controlling magnetic field B_0 away from the y-direction, i.e., the angle θ between B_0 and the plane of the qubit-NAMR loop cannot be zero strictly. Thus the nonzero component of B_0 in the z-direction

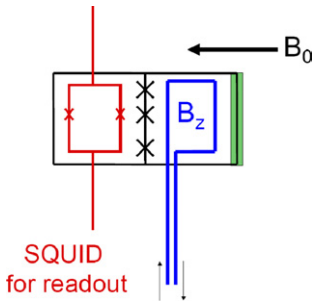

Figure 7. The unexpected vibration-induced fluctuation in the bias magnetic field could be cancelled by feeding back the readout of the SQUID.

$B_0 \sin\theta \sim B_0\theta$ penetrating the loop causes qubit energy fluctuations and decoherence. Roughly speaking, this decoherence source is proportional to B_0. Therefore, one needs to optimize B_0 such that it is large enough to dominate the coupling but not too large to induce strong decoherence from the torsional vibration of the sample plane with respect to B_0.

On the other hand, we could also reduce the fluctuation of the bias magnetic field of flux qubit by improving the experimental set-up. For example, we could use an eight-shaped gradiometer qubit. By the modified structure of the flux (as shown in figure 7), we can cancel the uniform magnetic field fluctuations over the qubit in the z-direction. The magnetic field threading the loop of the flux qubit is measured by the readout SQUID. Then with suitable feedback to compensate the fluctuation mentioned above, the bias magnetic field in the qubit-NAMR loop can be stabilized. In this case, strong magnetic field is attainable by the off-chip coil. However, scaling up to many qubits is not so straightforward and needs further consideration.

Another possible solution to overcome the above obstacles is to prepare B_0 by a superconducting coil and fix it on the sample chip at the dilution temperature. This method has the advantages that the set-up of the proposed controllable coupling mechanism need not be modified and sufficient strong controlling magnetic field B_0 can be achieved.

8. Discussions and remarks

In summary, we propose a novel solid-state cavity QED architecture that can reach the 'strong coupling regime' based on a superconducting flux qubit and a NAMR. In this composite system, the quantized flexural mode of the NAMR is coupled with the persistent current generated in the superconducting loop. The coupling strength can be independently modulated by an external magnetic field. We study the entangled energy spectrum of this composite system and find that a QND measurement of the flux qubit can be made in the dispersive limit. This composite system can be scaled up and the coupling mechanism can be extended to the case that the superconducting junction is a multi-level system. We also carefully examine the practical issues for experimental realization. The controllable strong coupling and the scalability enable coherent control over this system for quantum information processing as well as quantum state engineering. Besides, this cavity QED architecture offers a new scenario to demonstrate the intriguing phenomena of quantum optics in a solid-state quantum device. It also provides a possibility to test the quantization effect of mechanical motion.

Acknowledgments

This study is supported by the NSFC with grant numbers 90203018, 10474104, 60433050 and NFRPC with numbers 2005CB724508 and 2006CB921206. Y D Wang thanks J Q You and P Zhang for helpful discussions. This study is also partly supported by the JSPS-KAKENHI with grant numbers 16206003 and 18201018. KS thanks J Plantenberg, C J P M Harmans and J E Mooij for helpful discussions.

References

[1] Blais A, Huang R S, Wallraff A, Girvin S M and Schoelkopf R J 2004 *Phys. Rev.* A **69** 062320
[2] Johansson J, Saito S, Meno T, Nakano H, Ueda M, Semba K and Takayanagi H 2006 *Phys. Rev. Lett.* **96** 127006
[3] Wang Y D, Zhang P, Zhou D L and Sun C P 2004 *Phys. Rev.* B **70** 224515
[4] Wang Y D, Wang Z D and Sun C P 2005 *Phys. Rev.* B **72** 172507
[5] Wilson-Rae I, Zoller P and Imamoglu A 2004 *Phys. Rev. Lett.* **92** 075507
[6] Hopkin A, Jacobs K, Habib S and Schwab K 2003 *Phys. Rev.* B **68** 235328
[7] Martin I, Shnirman A, Tian L and Zoller P 2004 *Phys. Rev.* B **69** 125339
[8] Zhang P, Wang Y D and Sun C P 2005 *Phys. Rev. Lett.* **95** 097204
[9] Zhou X and Mizel A 2006 *Phys. Rev. Lett.* **97** 267201
[10] Mooij J E, Orlando T P, Levitov L, Tian L, Wal C H v d and Lloyd S 1999 *Science* **285** 1036
[11] Orlando T P, Mooij J E, Tian L, van der Wal C H, Levitov L S, Lloyd S and Mazo J J 1999 *Phys. Rev.* B **60** 15398
[12] van der Wal C H, ter Haar A C J, Wilhelm F K, Schouten R N, Harmans C J P M, Orlando T, Lloyd S and Mooij J E 2000 *Science* **290** 773
[13] van der Wal C H, Wilhelm F K, Harmans C J P M and Mooij J E 2003 *Eur. Phys. J.* B **31** 111
[14] Saito S, Thorwart M, Tanaka H, Ueda M, Nakano H, Semba K and Takayanagi H 2004 *Phys. Rev. Lett.* **93** 037001
[15] Cleland A N 2002 *Foundations of Nanomechanics* (Berlin: Springer)
[16] Armour A D and Blencowe M P 2001 *Phys. Rev.* B **64** 035311
[17] Armour A D, Blencowe M P and Schwab K C 2002 *Phys. Rev. Lett.* **88** 148301
[18] LaHaye M D, Buu O, Camarota B and Schwab K C 2004 *Science* **304** 74
[19] Cleland A N and Roukes M L 1996 *Appl. Phys. Lett.* **69** 2653
[20] Roukes M L 2000 *Technical Report: Technical Digest of the 2000 Solid-state Sensor and Actuator Workshop*
[21] Huang X M H, Zorman C A, Mehregany M and Roukes M L 2003 *Nature (London)* **421** 496
[22] Schwab K C, Blencowe M P, Roukes M L, Cleland A N, Girvin S M, Milburn G J and Ekinci K L 2005 *Phys. Rev. Lett.* **95** 248901
[23] Knobel R G and Cleland A N 2003 *Nature (London)* **424** 291
[24] Gaidarzhy A, Zolfagharkhani G, Badzey R L and Mohanty P 2005 *Phys. Rev. Lett.* **94** 030402
[25] Yu Y, Han S, Chu X, Chu S-I and Wang Z 2002 *Science* **296** 889
[26] Martinis J M, Nam S, Aumentado J and Urbina C 2002 *Phys. Rev. Lett.* **89** 117901
[27] Geller M R and Cleland A N 2005 *Phys. Rev.* A **71** 032311
[28] Wang Y D, Gao Y B and Sun C P 2004 *Eur. Phys. J.* B **40** 321
[29] Husain A, Hone J, Postma H W C, Huang X M H, Drake T, Barbic M, Scherer A and Roukesa M L 2003 *Appl. Phys. Lett.* **83** 1240
[30] Lupascu A, Verwijs C J M, Schouten R N, Harmans C J P M and Mooij J E 2004 *Phys. Rev. Lett.* **93** 177006
[31] Aldridge J S, Knobel R S, Schmidt D R, Yung C S and Cleland A N 2001 *Proc. SPIE* **11** 4591
[32] Haroche S 1992 *Fundamental Systems in Quantum Optics* (New York: Elsevier)
[33] Mooij J E and Harmans C J P 2005 *New J. Phys.* **7** 219

[34] Mooij J E and Nazarov Y V 2006 *Nat. Phys.* **2** 169
[35] Wallraff A, Schuster D I, Blais A, Frunzio L, Huang R S, Majer J, Kumar S, Girvin S M and Schoelkopf R J 2004 *Nature (London)* **431**
[36] Serban I, Solano E and Wilhelm F 2006 *Preprint* cond-mat/0606734
[37] Goorden M C, Thorwart M and Grifoni M 2004 *Phys. Rev. Lett.* **93** 267005
[38] Chiorescu I, Bertet P, Semba K, Nakamura Y, Harmans C J P M and Mooij J E 2004 *Nature (London)* **431** 159
[39] Saito S, Meno T, Ueda M, Tanaka H, Semba K and Takayanagi H 2006 *Phys. Rev. Lett.* **96** 107001
[40] Chiorescu I, Nakamura Y, Harmans C J P M and Mooij J E 2003 *Science* **299** 1869
[41] Bertet P, Chiorescu I, Burkard G, Semba K, Harmans C J P M, DiVincenzo D P and Mooij J E 2005 *Phys. Rev. Lett.* **95** 257002
[42] Bertet P, Chiorescu I, Semba K, Harmans C J P M and Mooij J E 2004 *Phys. Rev.* B **70** 100501
[43] Braginsky V B and Khalili F Y 1992 *Quantum measurement* (Cambridge: Cambrige University Press)
[44] Siddiqi I, Vijay R, Pierre F, Wilson C M, Metcalfe M, Rigetti C, Frunzio L and Devoret M H 2004 *Phys. Rev. Lett.* **93** 207002
[45] Siddiqi I, Vijay R, Metcalfe M, Boaknin E, Frunzio L, Schoelkopf R J and Devoret M H 2006 *Phys. Rev.* B **73** 054510
[46] Lupascu A, Driessen E F C, Roschier L, Harmans C J P M and Mooij J E 2006 *Phys. Rev. Lett.* **96** 127003
[47] Lupascu A, Saito S, Picot T, Groot P C d, Harmans C J P M and Mooij J E 2006 *Preprint* cond-mat/0611505
[48] Greywall D S, Yurke B, Busch P A, Pargellis A N and Willett R L 1994 *Phys. Rev. Lett.* **72** 2992
[49] Blencowe M and Wybourne M 1999 *Physica* B **280** 555
[50] Zhang Y and Blencowe M 2001 *J. Appl. Phys.* **91** 4249
[51] Schwab K 2001 *Proc. 1st Int. Conf. on Experimental Implementation of Quantum Computing*, ed R Clark p 189
[52] Buks E, Arbel-Segev E, Zaitsev S, Abdo B and Blencowe M P 2006 *Preprint* quant-ph/0610158
[53] Makhlin Y, Schoen G and Shnirman A 2001 *Rev. Mod. Phys.* **73** 357
[54] Raimond J, Brune M and Haroche S 2001 *Rev. Mod. Phys.* **73** 565
[55] You J Q, Nakamura Y and Nori F 2005 *Phys. Rev.* B **71** 024532
[56] Liu Y-x, You J Q, Wei L F, Sun C P and Nori F 2005 *Phys. Rev. Lett.* **95** 087001
[57] Liu Y-x, Wei L F, Tsai J S and Franco N 2006 *Phys. Rev. Lett.* **96** 067003
[58] Bergmann K, Theuer H and Shore B W 1998 *Rev. Mod. Phys.* **70** 1003
[59] Siewert J, Brandes T and Falci G 2005 *Preprint* cond-mat/0509735
[60] Majer J B, Paauw F G, Haar A J t, Harmans C J P and Mooij J E 2005 *Phys. Rev. Lett.* **94** 090501